

# Hyperbolic Horn Helical Mass Spectrometer (3HMS)

James G. Hagerman

Hagerman Technology LLC & Pacific Environmental Technologies

April 2005

## ABSTRACT

This paper describes a new type of mass filter based on the REFIMS (rotating electric field mass spectrometer) originally proposed by Clemmons [1] and later patented by Smith [2]. A clever and novel concept, the REFIMS has the advantage of parallel spectral readout, thanks to a two-dimensional detector plane. Unfortunately, it also has severe inherent problems relating to ion entrance angle and sensitivity making it practically unusable. The proposed 3HMS offers solutions to these difficulties with an innovative change to the structure.

## BACKGROUND

The REFIMS is a mass spectrometer similar to a quadrupole in the fact that four (or more) grid rods are used to channel and deflect an ion traveling down its center. The difference is that the RF field is driven on both pairs of grids in phases of 90 degrees apart, in effect "rotating" the electric field vector about the z-axis. No dc potentials are used. The resulting ion trajectory is a helical path, with a radius depending on operating voltage, frequency, and mass. Heavy ions will travel relatively undeflected down the center, light ions will crash into the grids. A "resonant" ion will achieve a fixed radius that can be detected by a Faraday cup or ring of equal radius, or a 2D plane array. Figure 1 shows the basic configuration.

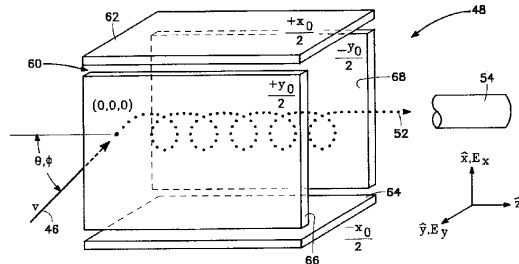


Fig 1. REFIMS construction and ion trajectory.

The major drawback to this device is the ion entrance requirements. The abrupt transition from free-space to the RF electric field between grids requires that the ion entrance angle, offset, and timing coincide with the resonant helical path at an exact RF phase. Another way to look at this is by reversing time. A resonant ion exiting the grids would travel out at a particular angle and offset radius. Constructing a device with these limitations is possible, but the loss of sensitivity is remarkable. Only ions entering the chamber at the exact RF phase will resonate, all others are rejected, even if of the correct mass. If this tolerance is +/-1 degree, it means a sensitivity loss of 180 times, even before filtering takes place.

## SOLUTION

The 3HMS offers a solution to the entrance angle problem. The idea is to compensate the electric field strength such that the ion helical radius starts at zero and linearly increases to the desired value, forming a spiral. This is accomplished by changing the grid shape from a fixed diameter tunnel to that

of a horn. Looking like the bell of a trumpet, the 3HMS horn has an effectively zero-strength electric field at its entrance, and hence, no ion deflection. As the grid spacing is reduced along the z-axis, the field strength increases proportionally, as does the helical radius. At the exit of the horn, the correct angle, offset, and timing are exactly achieved for driving a REFIMS. However, it is observed that the REFIMS is no longer needed, as the 3HMS provides the mass separation itself, without any loss of sensitivity. A subsequent benefit is the simplicity of bore-sighted construction.

## DESIGN

The helical trajectory of ion motion within a REFIMS is a sine function in both x and y dimensions. Acceleration along the z-axis is zero. Mathematical derivation in the xz plane is given by

$$x(z) = \frac{-q \cdot V}{m \cdot \omega^2 \cdot r_0} \cdot \cos(\omega \cdot t),$$

where  $r_0$  is the radius of the grid tunnel, and  $V$  is the amplitude of RF voltage. It can be seen that electric field strength is inversely proportional to  $r_0$ . Therefore, if we set

$$r_0 = \frac{1}{z},$$

the resulting field strength increases linearly with distance along the z-axis. This equation thus defines the shape of the 3HMS tunnel, as shown in Figure 2.

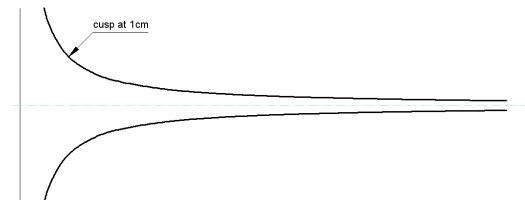


Fig 2. Hyperbolic shape of 3HMS horn.

Technically known as a rectangular hyperbola, this function has the drawback of infinite radius at  $z = 0$ . Fortunately, in practice an approximation is good enough.

For this analysis, a "ten-two horn" is arbitrarily specified. That is, the cusp radius is ten times the exit radius, and maximum flare radius is two times the cusp. Length is ten times the cusp. This is shown to scale in Figure 2. For practicality, the cusp dimension is set to 1 centimeter. It is also important that the entrance xy plane is a grid held to zero potential. Ions enter through a small aperture.

Plotting isopotential lines reveals the resulting electric field. Figure 3 shows the increasing strength of the field as the ion travels along the z-axis.

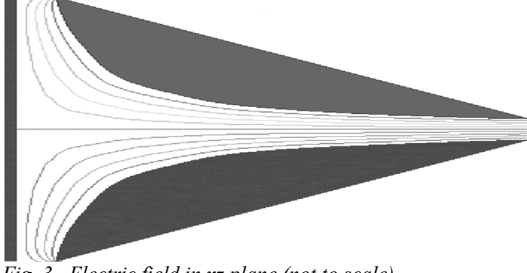


Fig. 3. Electric field in  $xz$  plane (not to scale).

The cross section is circular in shape. Although four grids are enough for proper operation, it is found that field linearity greatly improves when using eight grids, especially at larger radii. The cross section of a rotating field is shown in Figure 4.

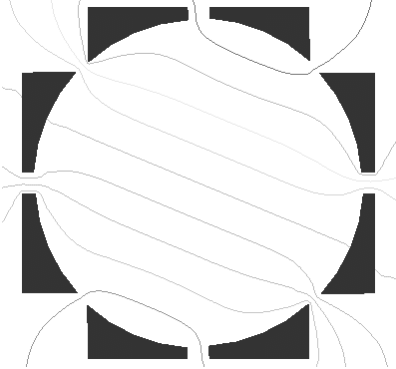


Fig. 4. Cross section electric field lines of octopole 3HMS.

#### ANALYSIS

Using mks units, the horn radius is redefined as

$$r = \frac{1}{\mu \cdot z},$$

where  $\mu$  is a conversion factor of  $100^2$ . This maintains the proper shape as specified but given in meters. The  $z$  position is related to time by

$$z = v \cdot t,$$

where velocity is

$$v = \sqrt{\frac{2 \cdot q \cdot E}{m}}.$$

$E$  is the potential voltage an ion is initially accelerated through. Once inside the 3HMS, the ion drifts at constant velocity along the  $z$ -axis (approximate, as will be shown later). The electric field between grids is given by

$$\Psi = \frac{V \cdot \cos(\omega \cdot t)}{r}.$$

The force on a charge is defined by

$$F = q \cdot \Psi$$

so the acceleration on a charged particle (ion) is

$$a = \Psi \cdot \frac{q}{m}.$$

To calculate position, combine the above equations and integrate acceleration twice in time.

$$a(t) = \frac{d^2x}{dt^2} = \frac{\mu \cdot v \cdot q \cdot V}{m} \cdot t \cdot \cos(\omega \cdot t).$$

Simplify first using the temporary substitution of

$$\lambda = \frac{\mu \cdot v \cdot q \cdot V}{m}$$

to get

$$\frac{d^2x}{dt^2} = \lambda \cdot t \cdot \cos(\omega \cdot t).$$

Integrating once obtains velocity.

$$\frac{dx}{dt} = \lambda \cdot \left[ \frac{\cos(\omega \cdot t)}{\omega^2} + \frac{t \cdot \sin(\omega \cdot t)}{\omega} \right].$$

Integrating again for position,

$$x(t) = \lambda \cdot \left[ \frac{2 \cdot \sin(\omega \cdot t)}{\omega^3} - \frac{t \cdot \cos(\omega \cdot t)}{\omega^2} \right].$$

In practice it is found that the first term, a constant amplitude sinewave, is insignificantly small and dominated by the second term. Ion position then simplifies and is rewritten as a function of  $z$  by

$$x(z) \approx -\frac{\mu \cdot q \cdot V}{m \cdot \omega^2} \cdot z \cdot \cos\left(\frac{\omega \cdot z}{v}\right).$$

This is the desired result. Amplitude increases linearly with  $z$ . Ion trajectory is plotted in Figure 5.

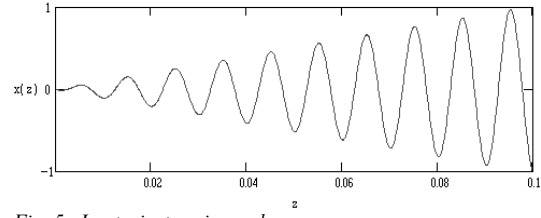


Fig. 5. Ion trajectory in  $xz$  plane.

#### PARAMETERS

Operational parameters are now considered by applying physical dimensions and units. Previously, the horn cusp was set at 1cm, giving an exit radius of 1mm. The derived ion trajectory equation is a sinewave having amplitude of

$$A = \frac{\mu \cdot q \cdot V \cdot z}{m_0 \cdot n \cdot (2 \cdot \pi \cdot f)^2}$$

and a number of cycles per length

$$C = \frac{f \cdot z}{v},$$

where

$$\omega = 2 \cdot \pi \cdot f$$

and

$$m = m_0 \cdot n.$$

Particle mass is the proton rest mass  $m_0$  times the number of protons  $n$  (amu). Operating parameters can be determined by arbitrarily forcing the number of helix turns to ten (one per cm). Solving our turns per length formula for frequency gives

$$f = \frac{v \cdot C}{z}$$

Substitute in the formula for velocity

$$f = \sqrt{\frac{2 \cdot q \cdot E}{m_0 \cdot n}} \cdot \frac{C}{z},$$

and it reduces to

$$f = (1.38 \cdot 10^6) \cdot \sqrt{\frac{E}{n}}.$$

Similarly, we force the exit amplitude to be equal to one-half the horn exit radius.

$$\frac{r}{2} = \frac{\mu \cdot q \cdot V \cdot z}{m_0 \cdot n \cdot 4 \cdot \pi^2 \cdot f^2}.$$

Solve for  $V$ , substitute in the solution for  $f$ , and it reduces to

$$V = \frac{r \cdot m \cdot 2 \cdot \pi^2 \cdot (1.38 \cdot 10^6)^2 \cdot E}{\mu \cdot q \cdot z}$$

or

$$V = (0.4) \cdot E.$$

## PRACTICE

Now that operating parameters have been reduced to simple functions of  $n$  and  $E$ , practical values for an actual device can be determined. The circuitry for producing RF signals up to 20V presently exist [4]. Thus, the ion accelerating voltage is set to 50V. A mass spectrum is thereby swept using frequency, related to amu ( $n$ ) by

$$f = \frac{(9.8 \cdot 10^6)}{\sqrt{n}}.$$

Figure 6 plots the relationship between amu and frequency.

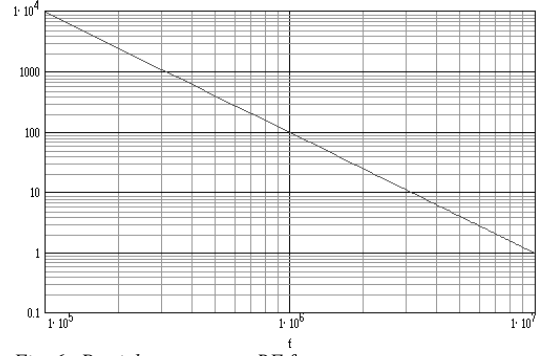


Fig. 6. Particle amu versus RF frequency.

## DETECTOR

A resonant ion is one that has an exit radius slightly less than the horn. Light ions will crash into the horn grids, heavy ions will propagate down the center at smaller radii. Therefore, detection of a resonant ion is done using a ring detector. Only ions exiting at a particular radius will be counted.

Another method is to use a disc-shaped detector that catches all heavy ions. This is akin to a low pass filter. As the frequency increases, so does collection current, creating essentially an integrated spectrum, appearing like a descending staircase. The knife-edge of the disc produces sharp transitions, however, the numerical differentiation required to produce a normal spectrum is plagued by noise.

A combined approach may achieve best results. With both disc and ring detectors, data are maximized for optimal post processing.

Positioning of the detectors is best done at a finite distance from the exit of the horn. This gives some magnification to the ion radius (similar to the flight into a REFIMS) and reduces centering errors. The exit angle is given by

$$\theta = \arctan\left(\frac{2 \cdot \pi \cdot r_i}{z_i}\right),$$

where  $r_i$  is the ion exit radius and  $z_i$  is the ion period, for an exit angle of 17 degrees.

## ERROR

One of the initial assumptions was that the acceleration along the  $z$ -axis is zero. This is not exactly correct, as there is bending of the electric fields lines, creating a  $z$  component to the field vector.

If a particle has a radius equal to the horn at exit, then it sees a reversing voltage equal to  $V$ . By setting "resonance" to half the horn exit radius, particle deceleration is  $V/2$ , or 10eV. Given an initial velocity of 50eV, this causes a decrease in ion velocity of 10%, diverging from predicted operation. The effect is that there will be approximately eleven helical cycles instead of ten, as the particle slows down.

Similarly, there is a corresponding increase, or restoration of velocity after the particle exits the horn, prior to striking the detector plane.

## IONIZATION

The entrance aperture and all grids in the 3HMS have no dc potentials. The creation of ions at a given velocity must be accomplished externally. Figure 7 shows one possible way of achieving this. A sample under test is pulled through a nozzle by the vacuum. The nozzle voltage is set to  $E$  (50V). Once molecules enter the chamber they are ionized and accelerated by the strong field produced by the grid. This grid is connected to a negative supply, perhaps  $-2kV$ . A small aperture in its center allows some ions to pass through towards the 3HMS, at ground potential, which decelerates the ions back to the exact 50eV required as they enter the horn.

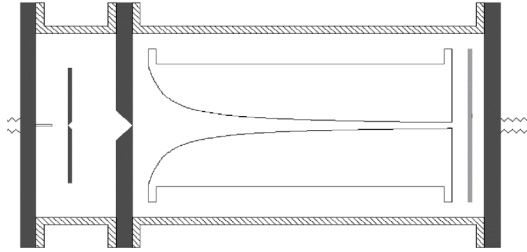


Fig. 7. 3HMS schematic with ionization chamber.

## SUMMARY

This paper described the principles of operation for a new type of mass spectrometer. Competitive in size and performance to a quadrupole, the 3HMS benefits from lower power RF voltages and the capability of two-dimensional spectral readout.

## REFERENCES

1. "Sounding Rocket Observation of Precipitating Ions in the Morning Auroral Region", Clemmons, 1992.
2. "Rotating Field Mass and Velocity Analyzer", Patent 5,726,448, Smith, 1997.
3. "Mass Spectroscopy Using a Rotating Electric Field", Clemmons, 1998.
4. "Aquasense: a Low-Power, High-Sensitivity, Portable Mass Spectrometer System for In Situ Measurement of Dissolved Gas and Solutes in Natural Waters, Atmospheric Gases and Aerosols, and Large Organic Compound Identification", PaceTech, 2003.

# Image Plane of 3HMS

James G. Hagerman

Hagerman Technology LLC & Pacific Environmental Technologies  
September 2005

## ABSTRACT

This paper describes the image plane of the new Hyperbolic Helical Horn Mass Spectrometer (3HMS). One of the primary benefits of this device is the capability of parallel spectral readout. That is, a portion of spectrum can be read at any instant, versus the common parameter sweeps over time. The image plane is two-dimensional, with each amu having a specific radial locus. A multi-element detector array can be designed to provide a linear-in-amu spectral readout.

## BACKGROUND

The original proposal for 3HMS [1] suggested a two-element detector system, the disc and ring. The center disc acts as a high-pass filter, collecting all ions not rejected by the rotating fields. As the operating parameters are changed, the resonant mass changes with either more or less ions striking the disc. Differentiating the resulting ion current (versus frequency) generates a valid spectrum. The knife-edge of the disc offers maximal resolution. Surrounding the disc is a separate ring detector. It collects only resonant ions, generating a proper spectrum directly.

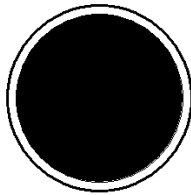


Fig. 1. Disc & ring detector array.

An improved detection scheme capable of exploiting the two-dimensional imagery for parallel readout can be derived by rigorous analysis of the ion trajectory at exit.

## ANALYSIS

Figure 2 shows a plot of a resonant ion trajectory through a 3HMS. It is radially symmetric, and the path is that of a corkscrew (helix). As an ion exits the horn it continues on a tangential path. The greater the distance to the detector plane, the greater the magnification of the resonant radius, and the sensitivity to center offset error is reduced.

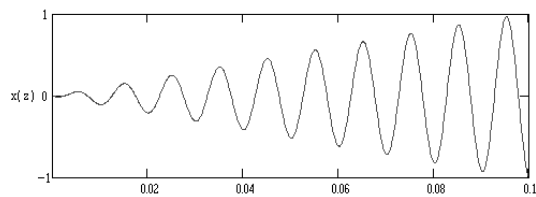


Fig. 2. Ion trajectory, side view.

The rotating electric fields at the exit of the horn assembly are just as critical as at the entrance. The field strength must be decreased as rapidly as possible to prevent further ion deflection. The best way to symmetrically do this is by

making the target plane a ground plane, having the same dc potential as the horn grids. This is easy to do since the electrometers used in detection are inherently grounded via feedback. Surrounding the Faraday collectors with a fixed ground completes the target image plane. Figure 3 shows the resulting field using isopotential lines.

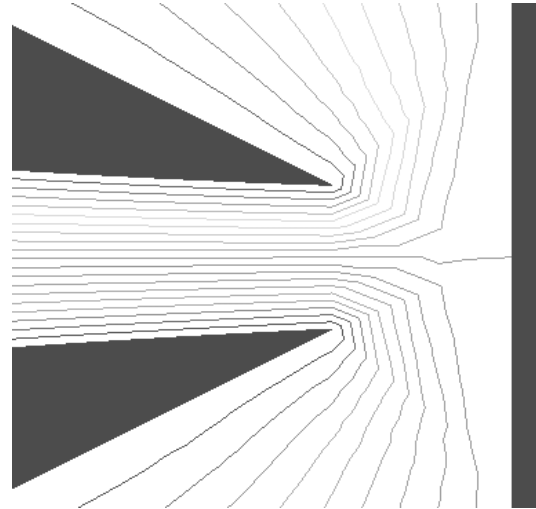


Fig. 3. Electric field between horn exit and image plane.

As it can be seen, the field strength rapidly decreases and changes direction. In fact, it is similar to the field at the horn entrance, but far more abrupt. Therefore, the effect on the ion is smoothly decreased to zero, to where the ion drifts freely. For this analysis, it is assumed that this is close enough to a free field that an ion continues tangentially to the velocity vector given the horn exit. Perhaps the fields can be improved by the addition of another grounded aperture right at the horn exit, or using a cup-shaped shield.

In any case, resonant ions exit the horn at a specific radius. The general formula for this trajectory is given [1] by

$$x(z) \approx -\frac{\mu \cdot q \cdot V}{m \cdot \omega^2} \cdot z \cdot \cos\left(\frac{\omega \cdot z}{v}\right)$$

Figure 4 shows the trajectories of various ion masses for a given set of operating conditions. The light ion crashes into horn grids; heavier ones pass through with decreasing exit angles.

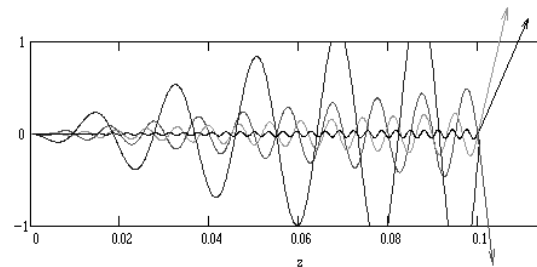


Fig. 4. Various ion masses through horn.

Calculating the exit angle is a little difficult, as the ions travel in a helix. That is, there will be some perpendicular axis offset, which effectively increases the resulting target radius. This can be seen looking down the z-axis.

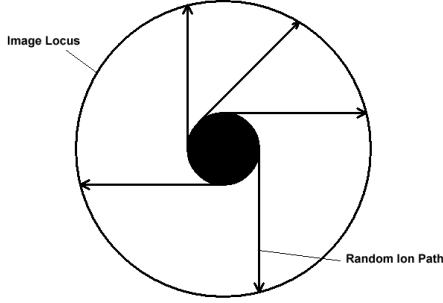


Fig. 5. Longitudinal view of ion paths to image plane.

Lengthening the drift distance  $d$  minimizes the error contributed by the offset, and for now will be ignored. The exit angle is simplified to the case shown in Figure 6.

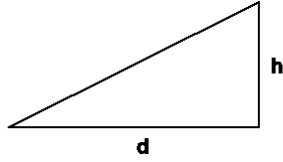


Fig. 6. Exit angle between horn and detector target.

To calculate the exit angle for any given ion mass, we differentiate our previous solution for trajectory.

$$\tan \theta = \frac{h}{d} = \frac{dx(z)}{dz} = \frac{d}{dz} \left[ -\frac{\mu \cdot q \cdot V}{m \cdot \omega^2} \cdot z \cdot \cos\left(\frac{\omega \cdot z}{v}\right) \right]$$

This solves as

$$\frac{h}{d} = \left( \frac{\mu \cdot q \cdot V}{m \cdot \omega \cdot v} \right) \cdot z \cdot \sin\left(\frac{\omega \cdot z}{v}\right)$$

Thanks to rotational symmetry, the sine term can be dropped. We then substitute the solution for  $v$ , and the angle reduces to

$$\frac{h}{d} = \frac{\mu \cdot V \cdot z}{\omega} \sqrt{\frac{q}{2 \cdot m \cdot E}}$$

The height  $h$  is the target radius at a given distance  $d$ . All of the other parameters are known or can be set to desired values. Using the values calculated in the 3HMS paper [1]:

$$\begin{aligned} z &= 0.1 \\ E &= 50 \\ V &= 20 \\ \mu &= 100^2 \\ m &= n \cdot 1.67 \cdot 10^{-27} \\ q &= 1.6 \cdot 10^{-19} \\ \omega &= 2 \cdot \pi \cdot f \end{aligned}$$

where  $n$  is the amu count, we arbitrarily set  $d$  to 5mm (0.005m). The target radial height  $h$  reduces to

$$h = \frac{15,600}{f \cdot \sqrt{n}}$$

At a frequency of 3.1MHz, we find the ion with  $n = 10$  to be resonant. Figure 7 plots the resulting radii at this frequency.

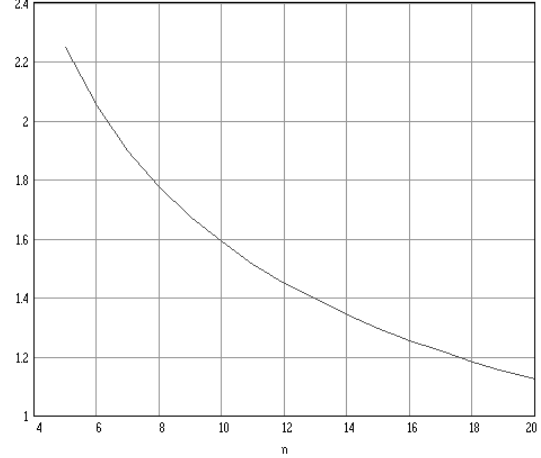


Fig. 7. Target height versus amu, scale in mm.

We now have a general solution for using a plane array detector at any given distance from the horn exit. Ion radius is proportional to the inverse root of  $n$ . Resolution is reasonable only over a small range, as the heavier ions have an asymptotic solution (zero radius). In the example above, a detector would be practical for parallel spectral readout from about 5 amu to 15 amu.

## DETECTOR ARRAY DESIGN

Taking the disc & ring detector concept further, we can place additional rings concentrically, each having a greater radius. This is shown in Figure 8. For a convenient linear-in-amu readout, the radii should have the same square root function as determined above. Such non-linear spacing then results in a perfect parallel spectral readout, using a minimum of detectors.

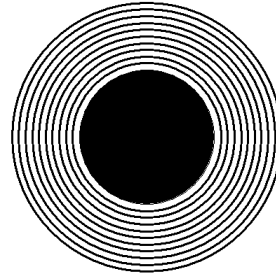


Fig. 8. Multiple ring detector architecture.

## CCD TYPE ARRAY

Recent technical advances have made the use of CCD devices practical as ion detectors. Some may be tempted to use a standard two-dimensional CCD type array structure for a detector. This is possible, but does not take advantage of the inherent rotational symmetry of the image plane. A price is paid in complexity, overhead, and efficiency. There is an

overwhelming increase in data, proportional to the number of pixels squared. Comparatively, a simple ten-ring detector is the equivalent of a 100 pixel CCD type array. There is a computational penalty for grid decomposition into polar coordinate, summation, and translation of non-linear response to amu. Sensitivity is also partially lost due to charge being spread out over many pixels, instead of just one.

Changing the array structure can alleviate all these problems. Rather than using a rectangular array, one could design a custom CCD using a single readout row in the shape of a spiral, as shown in Figure 9. The radius of such a spiral would be non-linear, following the inverse root function described above. The result would be an extremely fast parallel readout, linear in amu, and having very high spatial resolution.

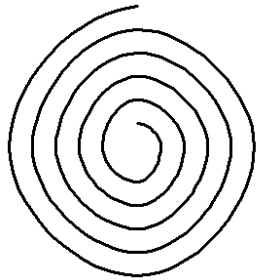


*Fig. 9. Spiral shaped CCD topology.*

## SUMMARY

This paper described the image plane of a 3HMS and appropriate detector array designs. Parallel spectral readout offers speed and throughput benefits for many areas of study. The ability to zoom in on specific peaks quickly and measure just spectral portions is acceptable for applications such as bomb detection or toxic gas monitoring.

## REFERENCES

1. "Hyperbolic Horn Helical Mass Spectrometer (3HMS)", Hagerman, 2005.
2. "Rotating Field Mass and Velocity Analyzer", Patent 5,726,448, Smith, 1997.